Fronts, Domain Growth and Dynamical Scaling in a d = 1 non-Potential System

R. Gallego, M. San Miguel and R. Toral
*Instituto Mediterráneo de Estudios Avanzados, IMEDEA * (CSIC-UIB)*
Campus Universitat de les Illes Balears, E-07071
Palma de Mallorca, Spain
(today)

We present a study of dynamical scaling and front motion in a one dimensional system that describes Rayleigh-Bénard convection in a rotating cell. We use a model of three competing modes proposed by Busse and Heikes to which spatial dependent terms have been added. As long as the angular velocity is different from zero, there is no known Lyapunov potential for the dynamics of the system. As a consequence the system follows a non-relaxational dynamics and the asymptotic state can not be associated with a final equilibrium state. When the rotation angular velocity is greater than some critical value, the system undergoes the Küppers-Lortz instability leading to a time dependent chaotic dynamics and there is no coarsening beyond this instability. We have focused on the transient dynamics below this instability, where the dynamics is still non-relaxational. In this regime the dynamics is governed by a non-relaxational motion of fronts separating dynamically equivalent homogeneous states. We classify the families of fronts that occur in the dynamics, and calculate their shape and velocity. We have found that a scaling description of the coarsening process is still valid as in the potential case. The growth law is nearly logarithmic with time for short times and becomes linear after a crossover, whose width is determined by the strength of the non-potential terms.

PACS:47.20.-k, 47.54.+r, 05.70.Ln

arXiv:cond-mat/9711217v1 21 Nov 1997

I. INTRODUCTION

A noteworthy result in the study of non-equilibrium statistical mechanics is the existence of dynamical scaling during the coarsening process in which a system approaches equilibrium after undergoing a phase transition [1,2]. Dynamical scaling reflects that domain growth is self-similar with a single time dependent characteristic length. In the simplest case of a relaxational dynamics for a scalar order parameter, which models, for example, an order-disorder transition (model A in the taxonomy of [3]), domains of two equivalent phases grow locally from an unstable state, and the approach to a final equilibrium state is dominated by interface motion. For spatial dimension $d > 1$, the mechanism for domain growth is curvature driven interface motion. This leads to a characteristic length growing as $R \sim t^{1/2}$. This type of phenomena has been studied in a large variety of systems which share the common feature that the final state of the dynamics is a state of thermodynamic equilibrium which minimizes a free energy or "potential" of the problem. Transient dynamics might also include additional processes beyond pure relaxation in that potential [4,5], but a measure of relative stability between stationary states is guaranteed by the existence of the potential. A more genuine non-equilibrium dynamics occurs when such a potential does not exist. A natural question, which we address in this paper, is the existence of dynamical scaling in the approach to a final stationary state which does not follow the minimization of a potential, while this transient dynamics from an unstable state involves the formation of spatial domains. The question of dynamical scaling can also be addressed for Hamiltonian dynamics [6], which is the extreme opposite situation to that of dissipative relaxational dynamics in a potential. A general non-equilibrium situation will, in general, have contributions from both types of dynamics [4,5].

The motion of an interface between two linearly stable solutions of a dynamical system was long ago proposed as a measure of relative stability for a non-potential system [7], and the motion of interfaces, domain walls or front solutions has been studied in a number of non-potential systems [8–11]. It is known that a domain wall between two equivalent states with different broken symmetry can move in $d = 1$ in either direction due to non-potential dynamics [8]. Likewise, non-potential dynamics can stabilize front solutions which, in the potential limit, would move from a globally stable into a metastable state [10]. It is the purpose of this paper to study the consequences of interface motion driven by non-potential dynamics on coarsening processes and dynamical scaling, which have been by and large not considered.

---

*URL: http://www.imedea.uib.es/PhysDept

A physical prototype situation in which the question posed above can be studied is Rayleigh-Bénard convection in a rotating cell [12], which in many aspects is mathematically equivalent to a biological model of competition between three species [13,14]. Beyond a threshold value for the parameter, δ, measuring the strength of non-potential terms (related to the rotation speed in the case of Rayleigh–Bénard convection) an instability to a time dependent dynamics occurs (Küppers-Lortz instability [15,16]). Below this instability, but still taking the system beyond the Rayleigh–Bénard convective instability, locally ordered domains, associated with different orientations of the convective rolls emerge. The subsequent coarsening process seems to be stopped by the Küppers-Lortz instability in $d = 2$ [17,18]. However, below the instability to a time dependent state, three preferred orientations exist and the motion of interfaces separating them is subject to non-potential dynamics which will affect domain growth.

With this motivation in mind, and as a first step towards the understanding of the problem of domain growth and dynamical scaling in this type of systems, we have considered a $d = 1$ model for three competing real non-conserved order parameters with the non-potential dynamics of [13,16] and spatial inhomogeneities determined by short range self-interactions. We have chosen this system because dynamical scaling in $d = 1$ potential systems is a special case for which well established results are available [2]: for the simplest case of a scalar non-conserved order parameter with short range interactions, a scaling solution is known with a logarithmic growth law for the typical domain size, $R \sim \log t$ [19,20]. This regime follows an early time regime of domain formation with a growth law $R \sim t^{1/2}$ [21]. The logarithmic domain growth has its origin in the interactions between domain walls [22]. The velocity of domain wall motion in these circumstances can be calculated by a perturbation analysis [23]. We study how these results are modified by non-potential dynamics. We find that dynamical scaling still holds, but with a crossover between two well defined regimes characterized by a logarithmic and linear domain growth law respectively. The two growth laws can be traced back to the two mechanisms that determine domain wall motion. The first one is the interaction between domain walls as in the potential case. The second one is due to the fact that the non-potential dynamics causes that isolated individual fronts move with finite velocity. In a multi-front configuration this provides and additional coarsening mechanism in which fronts moving in opposite directions annihilate each other. The crossover time between the two dominant mechanisms described depends on the strength of non-potential terms. When these become large enough, the logarithmic regime is pushed to just the very early times. In this case finite size effects become also important since very large domains emerge rather fast.

The outline of the paper is as follows: in section II we introduce the non-potential model and describe its homogeneous stationary solutions. In section III we clasify non-homogeneous front solutions and compute their velocity. We also analyze the interactions between two fronts including the non-potential effects. In section IV we discuss the issue of dynamical scaling and present numerical simulations that show the validity of the dynamical scaling description when non-potential terms are present. Finally, in section V we end with some conclusions and an outlook.

II. THEORETICAL MODEL

We base our theoretical approach in a three mode model first proposed in the context of fluid dynamics by Busse and Heikes [16]. In this model, the (real) amplitudes of the three selected modes corresponding to three different orientations of the convection rolls, A_1, A_2, A_3, follow the evolution equations:

$$\begin{aligned}
\partial_t A_1 &= A_1 \left(1 - A_1^2 - (\eta + \delta)\, A_2^2 - (\eta - \delta)\, A_3^2\right) \\
\partial_t A_2 &= A_2 \left(1 - A_2^2 - (\eta + \delta)\, A_3^2 - (\eta - \delta)\, A_1^2\right) \\
\partial_t A_3 &= A_3 \left(1 - A_3^2 - (\eta + \delta)\, A_1^2 - (\eta - \delta)\, A_2^2\right)
\end{aligned} \tag{2.1}$$

A similar set of equations was proposed earlier to model the behavior of three competing biological species [13]. In this case, A_1, A_2 and A_3 stand for the population number of each species. For the fluid case, δ is related to the rotation speed such that $\delta = 0$ is the non-rotating case; the parameter η is related to other fluid parameters. The analysis of [16] and [13] shows that, for a certain range of the parameters η and δ (see next section) there are no homogeneous stable solutions and the dynamics tends asymptotically to a sequence of alternations of the three modes as shown in experiments. An unwanted feature of the previous model is that the alternation time is not constant, but increases with time, contrary to experiments where an approximately constant period is observed. Although Busse and Heikes proposed that the addition of small noise could stabilize the period [5,24], an alternative explanation considered the addition of spatially dependent terms to the previous equations. Although the symmetries that must satisfy the amplitude equations would imply that the spatially dependent terms should be of an specific form [25–27], it has been shown in [17] that these can be further simplified without altering the essentials of the problem. We choose in this

work the simplest diffusive form for the spatial depending terms, namely:

$$\begin{aligned}\partial_t A_1 &= \partial_x^2 A_1 + A_1\left(1 - A_1^2 - (\eta+\delta)\,A_2^2 - (\eta-\delta)\,A_3^2\right)\\ \partial_t A_2 &= \partial_x^2 A_2 + A_2\left(1 - A_2^2 - (\eta+\delta)\,A_3^2 - (\eta-\delta)\,A_1^2\right)\\ \partial_t A_3 &= \partial_x^2 A_3 + A_3\left(1 - A_3^2 - (\eta+\delta)\,A_1^2 - (\eta-\delta)\,A_2^2\right)\end{aligned} \tag{2.2}$$

which form the basis of our subsequent analysis. A similar set of equations for the modulus square of the amplitudes is introduced in reference [14] for some particular values of the parameters η, δ. Notice that the system is invariant under the following transformations:
a) $x \to x + x_0$, $t \to t + t_0$ (spatio-temporal translation symmetry)
b) $A_1 \to A_2,\ A_2 \to A_3,\ A_3 \to A_1$ (cyclic permutation symmetry)
c) $A_i \rightleftarrows A_j,\ \delta \to -\delta$, where $A_i,\ A_j$ are any two different amplitudes.
The previous analysis shows that A_1, A_2 and A_3 are "equivalent" (from the dynamical point of view) variables.

It is possible to split the dynamical equations into a potential and a non-potential contributions:

$$\partial_t A_i = -\frac{\delta \mathcal{F}}{\delta A_i} - \delta \cdot f_i, \qquad i = 1,2,3 \tag{2.3}$$

where the potential function $\mathcal{F}$ is given by:

$$\begin{aligned}\mathcal{F}[A_1,A_2,A_3] = -\int dx \Big\{ &\frac{1}{2}\left[(\partial_x A_1)^2 + (\partial_x A_2)^2 + (\partial_x A_3)^2\right] + \frac{1}{2}(A_1^2 + A_2^2 + A_3^2)\\ &-\frac{1}{4}(A_1^4 + A_2^4 + A_3^4) - \frac{1}{2}\,\eta\,(A_1^2A_2^2 + A_1^2A_3^2 + A_2^2A_3^2)\Big\}\end{aligned} \tag{2.4}$$

and the non-potential terms are:

$$\begin{aligned} f_1 &= A_1(A_2^2 - A_3^2)\\ f_2 &= A_2(A_1^2 - A_3^2)\\ f_3 &= A_3(A_2^2 - A_1^2)\end{aligned} \tag{2.5}$$

In the case $\delta = 0$ the dynamical flow is of type *relaxational gradient* [4,5], that is, there exists a Lyapunov functional ($\mathcal{F}$) that monotonically decreases in time. When $\delta \neq 0$, however, one cannot find generally such a functional and we say that the system is *non-potential*.

There exist two kinds of homogeneous solutions which are stable in some region of the parameter space spanned by η and δ. These are three "roll" solutions $A_i = 1,\ A_j = 0\ (j \neq i),\ i = 1,2,3$, and one "hexagon" solution $A_1 = A_2 = A_3 = 1/\sqrt{1+2\eta}$ (this solution requires $\eta > -1/2$). A linear stability diagram of these solutions is shown in figure 1. We have focused on the region labeled with the letter 'R' for rotation speeds below the Kuppers-Lortz instability ($|\delta| < \eta - 1$) and where the rolls are the stable solutions. In this region we expect the formation of domain walls connecting homogeneous stable roll solutions.

III. FRONT SOLUTIONS

A. Isolated fronts

In the context of the present study, fronts or domain walls are defects that connect two stable homogeneous solutions. Fronts in one dimension are usually termed *kinks* and we will often refer to them in this way. We focus on the spatial-dependent stationary solutions of (2.2) with $\delta = 0$. The stable kink solutions are such that one of the three amplitudes, say A_k, satisfying the boundary conditions $A_k(x \to \pm\infty) = 0$ is zero everywhere. In order to study the dynamics of the non-potential kinks, we first consider the kinks associated with the stationary potential problem and then we treat the non-potential terms as a perturbation. The two non-vanishing stationary amplitudes A_i and A_j are, for $\delta = 0$, solutions of:

$$\begin{aligned}\partial_x^2 A_i &= -A_i + A_i^3 + \eta\, A_i A_j^2\\ \partial_x^2 A_j &= -A_j + A_j^3 + \eta\, A_j A_i^2\end{aligned} \tag{3.1}$$

with boundary conditions $A_i(-\infty) = A_j(+\infty) = 0$ and $A_i(+\infty) = A_j(-\infty) = 1$.

The system (3.1) may be considered to represent the two dimensional motion of a Newtonian particle of unit mass ($x \to t$, $A_i \to X$, $A_j \to Y$) under the action of a force with potential function $V(X,Y) = \frac{1}{2}(X^2+Y^2) - \frac{1}{4}(X^4 + Y^4) - \frac{1}{2}\eta X^2 Y^2$. This function has two maxima in $m_0 = \{A_i = 1, A_j = 0\}$ and $m_1 = \{A_i = 1, A_j = 1\}$. It is clear that there exists a unique trajectory (allowed by the dynamics) along which a particle located in $m_0(m_1)$ can reach $m_1(m_0)$. The kink profile corresponds to the variation in time of the particle coordinates $(X(t), Y(t))$ when it moves between the two maxima [28].

An explicit analytical solution can be found in two particular cases [29]. First, when $0 < \eta - 1 \ll 1$, we have:

$$\begin{aligned} A_i^0(x) &= r(x)\ \left[1 + \exp\left(2\sqrt{\eta-1}(x-x_0)\right)\right]^{-1/2} \\ A_j^0(x) &= r(x)\, e^x\ \left[1 + \exp\left(2\sqrt{\eta-1}(x-x_0)\right)\right]^{-1/2} \end{aligned} \tag{3.2}$$

with $r(x) = 1 + (\eta-1)R(x),\ R(x) = O(1)$. Secondly, when $\eta = 3$ it is possible to obtain exact analytical solutions:

$$\begin{aligned} A_i^0(x) &= \frac{1}{1+e^{\mp\sqrt{2}(x-x_0)}} = \frac{1}{2}\left[1 \pm \tanh\left(\frac{x-x_0}{\sqrt{2}}\right)\right] \\ A_j^0(x) &= \frac{1}{1+e^{\pm\sqrt{2}(x-x_0)}} = \frac{1}{2}\left[1 \mp \tanh\left(\frac{x-x_0}{\sqrt{2}}\right)\right] \end{aligned} \tag{3.3}$$

In both cases x_0 is arbitrary but fixed. From these solutions it is clear that the spatial scale over which A_i^0 and A_j^0 vary is of order $1/\sqrt{\eta-1}$.

The three roll solutions are equivalent and they yield the same value for the Lyapunov functional (2.4). Therefore, we expect kinks not to move in the potential problem ($\delta = 0$). We now ask about the persistence of these kink solutions when δ is different from zero. For this we will use singular perturbation theory. Let us assume δ to be small, say of order ε, and look for a solution of (2.2) (with $A_k(x) = 0$) of the form:

$$\begin{aligned} A_i(x) &= A_i^0(x - s(t)) + \varepsilon\, A_i^1(x - s(t)) + O(\varepsilon^2) \\ A_j(x) &= A_j^0(x - s(t)) + \varepsilon\, A_j^1(x - s(t)) + O(\varepsilon^2) \end{aligned} \tag{3.4}$$

where $A_i^0(x)$ and $A_j^0(x)$ are solutions of (3.1). Substituting into (2.2) and matching the terms of the same order in ε, we find, at order $O(\varepsilon^0)$:

$$\begin{aligned} \partial_x^2 A_i^0 + A_i^0 - (A_i^0)^3 - \eta\, A_i^0 (A_j^0)^2 &= 0 \\ \partial_x^2 A_j^0 + A_j^0 - (A_j^0)^3 - \eta\, A_j^0 (A_i^0)^2 &= 0 \end{aligned} \tag{3.5}$$

and at order $O(\varepsilon^1)$:

$$\mathcal{L}\,\boldsymbol{\alpha} = \boldsymbol{\alpha}' \tag{3.6}$$

where

$$\mathcal{L} = \begin{pmatrix} \partial_x^2 + 1 - \eta\left[(A_i^0)^2 + (A_j^0)^2\right] & -2\eta A_i^0 A_j^0 \\ -2\eta A_i^0 A_j^0 & \partial_x^2 + 1 - \eta\left[(A_i^0)^2 + (A_j^0)^2\right] \end{pmatrix}$$

$$\boldsymbol{\alpha} = \begin{pmatrix} A_i^1 \\ A_j^1 \end{pmatrix},\ \boldsymbol{\alpha}' = \begin{pmatrix} \delta\varepsilon^{-1}(A_i^0)^2 A_j^0 - A_i^0 \partial_t s \\ -\delta\varepsilon^{-1} A_j^0 (A_i^0)^2 - A_j^0 \partial_t s \end{pmatrix}$$

The solvability condition for the existence of a solution $(A_i^1(x),\ A_j^1(x))$ reads

$$(\boldsymbol{\Phi}^\dagger,\ \boldsymbol{\alpha}') = 0 \tag{3.7}$$

where $(\cdot,\cdot)$ is a scalar product in $L^2(\mathbb{R})$ defined by $(f,g) = \int_{-\infty}^{\infty} dx f(x)^* g(x)$ and $\boldsymbol{\Phi}^\dagger$ belongs to the null space of the auto-adjoint operator $\mathcal{L}$. Because of the translational invariance, $\mathcal{L}$ has a zero eigenvalue so that its kernel is not empty. The associated eigenvector is generally known to be

$$\boldsymbol{\Phi}^\dagger = \begin{pmatrix} \partial_x A_i^0 \\ \partial_x A_j^0 \end{pmatrix} \tag{3.8}$$

This is immediately seen taking, for example, the derivative of (3.5) with respect to x. Eq. (3.7) can now be explicitly evaluated. From this equation , the solitary *kink velocity* in the non-potential case is obtained at leading order:

$$v(\delta) \equiv \partial_t s = \delta \, \frac{\int_{-\infty}^{\infty} dx \, A_i^0 A_j^0 \, (A_j^0 \, \partial_x A_i^0 - A_i^0 \, \partial_x A_j^0)}{\int_{-\infty}^{\infty} dx \, \left[(\partial_x A_i^0)^2 + (\partial_x A_j^0)^2 \right]} + O(\delta^2) \tag{3.9}$$

Therefore, in the non-potential case, the kink moves despite connecting states associated with the same value of the Lyapunov potential of the equilibrium problem, as already known for other problems [8]. For the particular case of $\eta = 3$ for which an analytical result is available for the kink profile, (eq. (3.3)), an explicit result is obtained for the solitary kink velocity, namely $v(\delta) = \delta\sqrt{2}/4$

The expression (3.9) gives not only the magnitude of the velocity but also the direction of motion, which is related to the sign of v. First, we note that the velocity is at leading order proportional to δ, so the direction of the motion depends upon the sign of δ. To illustrate how (3.9) determines the direction, let us consider for example a kink with boundary conditions: $A_i(-\infty) = A_j(+\infty) = 0$ and $A_i(+\infty) = A_j(-\infty) = 1$; $A_i^0(x)$ and $A_j(x)$ are such that $\partial_x A_i^0 > 0$ and $\partial_x A_j^0 < 0$. In this case the numerator of (3.9) is positive and v has the sign of δ. A positive (negative) value of v corresponds to a kink moving to the right (left). In figure 2 we show a classification of the six possible types of isolated kinks and their direction of motion. Three of them move in one direction and the other three in opposite direction.

We have checked numerically the domain of validity of the perturbative result (3.9) (see figure 3). To check (3.9) we either use the analytical result of the kink profile A_i^0 for $\eta = 3$, or, more generally, the kink profile A_i^0 obtained numerically. For a value of $\eta = 3.5$, we see that the perturbative result to first order in δ (3.9) turns out to be in good agreement with the numerical results approximately for values of $\delta \lesssim 1.5$. Of course this upper limit of validity depends on η in such way that it gets bigger as η is larger. Above this limit the linear relation between v and δ is no longer valid and one needs to compute further corrections in terms of successive powers of δ.

B. Multifront configurations

To study transient dynamics and domain growth we consider random initial conditions of small amplitude around the unstable solution $A_1 = A_2 = A_3 = 0$. In this situation a multifront pattern emerges rather than a solitary kink. In order to study dynamical scaling, we are interested in the late stage of this dynamics, once well-defined domains have been formed.

In a potential system governed by a non-conserved scalar order parameter with short range interactions, as it the case with $\delta = 0$, late time dynamics can be explained in terms of the interaction (and further annihilation) among adjacent kinks [14,19,20,22]. An isolated kink is stable. The interacting force between kinks turns out to be proportional to $\exp(-\alpha d)$ [22], where α is some *positive* constant related to the interface width and other system parameters, and d is the distance between two adjacent kinks. This interaction among kinks leads to a growth law for the characteristic length that depends on time logarithmically [19,20]. The force is attractive and leads to kink annihilation. The process occurs in such way that the domain that vanishes first is the smallest one. Kink annihilation occurs in a very small time scale. In fact, the hypothesis of "instantaneous annihilation" has been found to be a good assumption [19]. Kink annihilation induces domain coarsening leading to a final state with an homogeneous roll solution filling up the whole system.

When δ is different from zero the long stage dynamics should still be explained in terms of moving fronts which annihilate each other. But now two very distinct competing physical phenomena come into play. On the one hand, there is the aforementioned kink interaction. On the other hand, we have the kink motion driven by non-potential effects. In this case, we do not expect the growth law to be logarithmic, at least in the regime where the non-potential effects (the strength of which is measured by δ) are important. In figure (4) we show some snapshots corresponding to a typical run of the temporal evolution of the system (we use periodic boundary conditions). The first snapshot corresponds to an early stage during which domains are forming. Once formed, kinks move in such a way that annihilations of contrapropagating adjacent kinks leads to coarsening. Eventually, as corresponding to the last snapshot, the system may be in a state with a group of kinks moving all in the same direction. These will interact among them (with a interaction force that varies logarithmically with the interkink distance) until extinction.

We have performed a perturbation analysis of domain growth in the simplest example of a single domain bounded by two moving domain walls. A differential equation for the domain size $s(t)$ can be obtained in the general case (see appendix). For $\eta = 3$ it adopts the simple form:

$$\partial_t s(t) = 2v(\delta) - 24\sqrt{2} e^{-\sqrt{2} s(t)} \tag{3.10}$$

where $v(\delta)$ is the solitary kink velocity. This expression is obtained in the "dilute-defect gas approximation", that is, when the width of the fronts is much smaller than the distance between them. The first term in the right hand of (3.10) can be either negative or positive and represents the contribution to the variation of the domain size owing to non-potential effects. The second term is related to the interacting force between the kinks and it is always negative (attractive force) so that it tends to shrink the domain. If both terms are negative, the kinks will annihilate each other. Otherwise, when the first term is positive, the two effects act in opposite directions. In fact, given an initial size of the domain s_0, it is possible to find a value $\delta = \delta_c$ for which the domain neither shrinks nor grows; in this case, the initial domain would not evolve in time being a stationary solution. For values $\delta > \delta_c$ the domain would get wider whereas for $\delta < \delta_c$ it would shrink. Note that in the $\delta = 0$ case (potential regime), the isolated domain always collapses, but this can be stopped with a suitable strength of the non-potential terms. Furthermore, given a fixed value of δ, if s_0 is large enough, the dominant term responsible of the kink motion is the one associated with $v(\delta)$. In this case the fronts move at a constant velocity leading to a variation of the domain size linear with time. On the other hand, if s_0 is small enough, kink interaction will be the dominant effect and the single domain size will collapse logarithmically with time. This picture of the size dynamics of a single domain also explains basically what happens when more domains (and a non-vanishing third amplitude) coexist. It gives a useful understanding of the characteristic growth laws obtained from a statistical analysis in the next section.

IV. DOMAIN GROWTH AND SCALING

In this section we focus on the scaling properties of the system (2.2) in a late stage of the dynamics, namely when well-defined domains have formed. The scaling hypothesis states that there exists a single characteristic length scale $R(t)$ such that the domain structure is, in a statistical sense, independent of time when lengths are scaled by $R(t)$. We will refer to the time dependence of the scale length as the *growth law* of the system. It has been found that the scaling hypothesis holds in a great variety of potential systems. The system under study here gives us the opportunity of answering the question of whether a non-potential dynamics satisfies dynamical scaling.

Two magnitudes frequently used to study domain growth and scaling properties for a scalar field $\Psi(\mathbf{x}, t)$ (for instance, one of the three amplitudes in equations (2.2)) are the equal time correlation function

$$C(\mathbf{r}, t) = \left\langle \sum_{\mathbf{x}} \Psi(\mathbf{x}+\mathbf{r}, t)\Psi(\mathbf{x}, t) \right\rangle_{\text{i.c.}} \tag{4.1}$$

and its Fourier transform, the equal time structure factor

$$S(\mathbf{k}, t) = \left\langle \sum_{\mathbf{k}} \hat{\Psi}(\mathbf{k}, t)\hat{\Psi}(-\mathbf{k}, t) \right\rangle_{\text{i.c.}} \tag{4.2}$$

where the angular brackets indicate an average over initial conditions ("runs"). If a single characteristic length exists, according to the scaling hypothesis, the pair correlation function and the structure factor must have the following scaling forms in a d-dimensional system:

$$C(\mathbf{r}, t) = f(r/R(t)) \tag{4.3}$$

$$S(\mathbf{k}, t) = R(t)^d \hat{f}(kR(t)) \tag{4.4}$$

The function f is called the *scaling function*. To check numerically the validity of the previous scaling laws, we have integrated the system of equations (2.2) using a finite difference method for both, the spatial and temporal derivatives. In the simulations we have taken a constant value for η, namely $\eta = 3.5$, and we have varied δ from $\delta = 0$ (potential case) to $\delta = 0.1$ (a value below the KL instability threshold). We have used periodic boundary conditions and have averaged our results over 100–500 runs and used system sizes ranging from $L = 250$ to $L = 1000$. To study domain structure, we consider the correlation function of one of the three amplitudes. We use the correlation function better than the structure factor because of the large fluctuations of the structure factor at small wave numbers. A typical length scale associated with the average domain size can be defined in several ways. Specifically, we have determined it by computing the value of r for which $C(r, t)$ is half its value at the origin at time t, that is $C(R(t), t) = \frac{1}{2}C(0, t)$. The calculation has been performed by fitting the four points of $C(r, t)$ closest to $C(0, t)$ to a cubic polynomial. Another typical length, $R_1(t)$ can be evaluated directly as the system size divided by the number of kinks. We have verified that the quotient $R_1(t)/R(t)$ remains nearly constant, as expected, when a single characteristic length dominates the problem.

A. Growth Law

We consider first the potential case $\delta = 0$: In figure 5 we show that the domain size follows the expected logarithmic behavior. The attractive interaction among the kinks leads to a very long transient before the system reaches its final state which corresponds to one roll solution filling up the whole system.

In the non-potential case the domain size $R(t)$ is shown in figure 6 for a system of size 500 and $\delta = 10^{-3}$. For the earliest times, when the kinks are very close to each other, and according to the discussion in section III B we expect the interaction terms to be the dominant ones (as long as δ is small enough). This leads to a logarithmic growth of $R(t)$ as observed in region (α) of figure 6. Due to coarsening the characteristic domain size becomes larger and the domain wall interaction becomes weaker as the time increases. For longer times the non-potential effects dominate with respect to wall interaction. In this regime we can consider each domain wall to move at a constant velocity. This gives rise to a linear behavior of $R(t)$ with time (region (γ)). Between regions (α) and (γ) there exists a crossover (region (β)) for which the weights of both effects (interaction and non-potential) in driving the domain wall motion are of the same order. Finally, at very late times finite size effects come into play (region (δ)): the domain size saturates to a constant value and the number of domain walls is too small to make good statistics.

In the regime for which the interaction effects are the dominant ones, we can give a simple explanation of the linear growth law observed for $R(t)$. Statistically speaking, there will be the same number of kinks moving to the right and to the left. As a matter of fact, in an appropriate reference frame, the system can be seen as composed of motionless kinks (type 1) and kinks moving at a velocity of $2v$ in one fixed direction (type 2) . If we call $N_1(t)$ and $N_2(t)$ the *average* number of kinks of both types at time t, the number of kinks of, say type 1, at time $t + dt$ will be:

$$N_1(t + dt) = N_1(t) - N_1(t)\, v\, dt \times \frac{N_2(t)}{L} \tag{4.5}$$

where the second term in the right hand side represents the number of kinks disappeared in dt by annihilation and L stands for the system size. The important point is that $N_1(t) = N_2(t) = N(t)$ (remember we are dealing with averaged quantities), so that (4.5) transforms into:

$$\frac{dN(t)}{dt} = 1 - \frac{v}{L} N(t)^2 \tag{4.6}$$

The integration of the previous equation gives $N(t) = [(v/L)t + N_0^{-1}]^{-1} \sim t^{-1}$, so that the average inter-kink distance $R(t) \sim N(t)^{-1} \sim t$ is linear with time.

When δ is large enough the initial kink annihilation is so fast that the regions (α) and (β) in the $R(t)$ plot can hardly be observed in the numerical integration. In this case of large non-potential effects, a linear growth law is observed for the shortest times and it continues until finite size effects show up clearly (see figure 7). Finite size effects are seen to occur for $t > 200$ for $\delta = 0.1$. The bigger δ, the sooner finite size effects appear.

At long times the system will consist of an homogeneous roll state or a group of kinks moving either to the right or to the left [31]. Note that the periodic boundary conditions impose constraints about the number of such moving kinks. To be precise, the number of kinks moving in a fixed direction must be multiple of three. We can form a subgroup of three kinks moving in the same direction by joining those appearing in each row of figure (2). The moving kinks will carry on interacting among them (logarithmically) until eventually they all will disappear. In this situation we expect the growth law to be logarithmic with time but one of such groups is composed typically of three, six or rarely nine kinks, a number too small as to make good statistics.

B. Scaling function

We now address the question of the validity of the dynamical scaling hypothesis (4.3). For this purpose, we have plotted the equal time correlation function $C(r, t)$ versus the scaled length $r/R(t)$ for several times. Figure 8 shows the scaling function in the potential case. In figures 9 and 10 we show the correlation functions for several times before and after scaling the system length. Our results show that the correlation functions follow a single profile when the length is scaled with the characteristic domain sizes obtained above. We therefore conclude that a scaling description of the system is also valid as in the potential case, but now with a non-potential dynamics. The upper limit of the time interval during which there is scaling is determined by the appearance of finite size effects. The range of values of δ for which there is scaling in a quite large time interval is rather small. For values of δ even of a few tenths, the finite size effects show up for very short times. Moreover the fluctuations in the scaling function grow as δ increases. For these reasons, we have not been able to obtain a conclusive comparison among scaling functions for different values of δ, although their shapes appear to be rather insensitive to the value of δ.

V. CONCLUSIONS

We have studied domain growth and dynamical scaling in a non-potential coarsening process in one dimension. The model considered is motivated by the phenomenon of Rayleigh-Bénard convection in a rotating cell. We have focused on the region below the Küppers-Lortz instability point, where the dynamics is still non-potential and the system shows coarsening. A solitary kink moves at a constant velocity due to the non-potential dynamics. When there are several kinks present in the system, these move due to both, domain wall interaction and non-potential effects. In any case the dynamics is governed by motion of interfaces. This motion is such that kinks moving in opposite directions annihilate each other. As a consequence of kink annihilation the average domain size grows in time and the system coarsens. When $\delta = 0$ (potential case) we have shown that, in accordance with general results, the growth law is logarithmic with time and that a scaling description of the system dynamics is possible. When δ becomes different from zero we have found that the scaling hypothesis still holds, as in the potential case, but with a different growth law that reflects the non-potential dynamics of the system. For the shortest times, the kink interaction (the only effect present in the potential case) is the dominant effect and gives rise to a logarithmic growth law with time. For longer times the average inter-kink distance is large enough to make the interaction effects negligible in driving kink motion. Therefore each kink moves nearly independently of the others as if it were isolated. In this situation each kink moves with a constant velocity leading to a linear growth law. For larger values of δ the logarithmic region is not observed because of the fast annihilation of the domains during the very early times. The two dimensional version of this problem is currently under study [32] and it exhibits rather different dynamical behavior grossly dominated by vertices where three domain walls meet and which have no parallel in one dimensional systems.

APPENDIX

We consider an isolated domain bounded by two domain walls associated with amplitudes A_1 and A_2, while $A_3 = 0$. When the domain size is much greater than the interface width ("dilute-defect gas approximation"), a reasonable *ansatz* for this solution is

$$\begin{aligned} A_1(x,t) &= a(x - r(t)) + b(x - d + r(t)) + w_1(x,t) \\ A_2(x,t) &= b(x - r(t)) + a(x - d + r(t)) - 1 + w_2(x,t) \end{aligned} \tag{A.1}$$

where $r(t)$ measures the displacement of the kinks, d is the initial domain size (so that the domain size at time t is $d - 2r(t)$), $\partial_t r$ and w_i $(i = 1, 2)$ are assumed to be small corrections of order δ and $\partial_t w_i$ to be negligible with respect to w_i. To simplify notation, we use: $f \equiv f(x - r(t))$, $f_d \equiv f(x - d + r(t))$. The moving fronts a and b satisfy the boundary conditions $a(\infty) = b(-\infty) = 0$, $a(-\infty) = b(\infty) = 1$ and they are solutions of the system (2.2) (with one of the amplitudes equal to zero) so that the following equations hold:

$$\mathcal{M}_+(a,b) = \mathcal{M}_+(b_d, a_d) = \mathcal{M}_-(b,a) = \mathcal{M}_-(a_d, b_d) = 0 \tag{A.2}$$

where the action of the operators $\mathcal{M}_\pm(\cdot,\cdot)$ is given by:

$$\mathcal{M}_\pm(f,g) = \partial_x^2 \pm v(\delta)\partial_x + f - f^3 - (\eta \pm \delta) f g^2 \tag{A.3}$$

The parameter $v(\delta)$ is the front velocity as given by eq. (3.9).

Introducing the ansatz (A.1) into (2.2) we obtain, at leading order, a linear system of equations for w_1 and w_2:

$$\mathcal{L}\boldsymbol{\phi} = \boldsymbol{\phi}' \tag{A.4}$$

$$\mathcal{L} = \begin{pmatrix} \partial_x^2 + 1 - 3(a + b_d)^2 - \eta(b + a_d - 1)^2 & -2\eta(a + b_d)(a_d + b - 1) \\ -2\eta(a + b_d)(a_d + b - 1) & \partial_x^2 + 1 - 3(a_d + b - 1)^2 - \eta(a + b_d)^2 \end{pmatrix}$$

$$\boldsymbol{\phi} = \begin{pmatrix} w_1 \\ w_2 \end{pmatrix}, \quad \boldsymbol{\phi}' = \begin{pmatrix} (\partial_x a + \partial_x b_d)v(\delta) + (\partial_x b_d - \partial_x a)\partial_t r + K_1\delta + K_2\eta + K_3 \\ (\partial_x b + \partial_x a_d)v(\delta) + (\partial_x a_d - \partial_x b)\partial_t r + K_1'\delta + K_2'\eta + K_3' \end{pmatrix}$$

where the functions $K_i(x,t)$ and $K_i'(x,t)$ $(i=1,2,3)$ are given by:

$$\begin{aligned}
K_1 &= a(a_d-1)^2 + 2b(a+b_d)(a_d-1) + b_d(1-2a_d+b^2)\\
K_2 &= a(a_d-1)^2 + 2(a_d-1)(ab+a_db_d+bb_d) + b_d(1+b^2)\\
K_3 &= -2\,\partial_x^2 b_d + b_d(3a^2+3ab_d+2b_d^2-2)\\
K_1' &= -a(a+2b_d)(a_d-1) + b_d(b_d-2ab-bb_d)\\
K_2' &= a(a+2b_d)(a_d-1) + b_d(2ab+bb_d+2a_db_d-b_d)\\
K_3' &= -2\,\partial_x^2 a_d + 3b^2(a_d-1) + 3b(a_d-1)^2 + 2a_d^3 - 3a_d^2 + a_d
\end{aligned}$$

The solvability condition for the existence of a solution $(w_1(x,t), w_2(x,t))$ for (A.4) reads

$$(\mathbf{\Psi}^\dagger,\ \boldsymbol{\phi}') = 0 \tag{A.5}$$

where $\mathbf{\Psi}^\dagger$ belongs to the kernel of the auto-adjoint linear differential operator $\mathcal{L}$. We will show below that $\mathbf{\Psi}^\dagger$ is approximately given by $(\partial_x a,\ \partial_x b)^T$ (here T denotes the transposed vector), where $a = a(x-r(t))$ and $b = b(x-r(t))$ are the domain wall profiles around $x = r(t)$.

The first component of the vector $\mathcal{L}\mathbf{\Psi}^\dagger$ is given by:

$$\begin{aligned}
(\mathcal{L}\mathbf{\Psi}^\dagger)_1 &= \mathcal{L}_{11}\partial_x a + \mathcal{L}_{12}\partial_x b\\
&= \partial_x^3 a + \partial_x a - 3(a+b_d)^2\partial_x a - \eta(a_d+b-1)^2\partial_x a - 2\eta(a+b_d)(a_d+b-1)\partial_x b
\end{aligned} \tag{A.6}$$

As long as that the width of the interfaces is much smaller than the domain size (for all times t), we can make the following approximations: $ab_d \approx 0,\ aa_d \approx a,\ bb_d \approx b_d$. Moreover, this assumption implies that the product of the derivative with respect to x of an amplitude solution centered on $x = x_0$ multiplied by another amplitude shifted a length of order of the domain size, will be a function which will take values different from zero only in a small region around $x = x_0$. By using the approximations

$$\begin{aligned}
(a+b_d)^2\partial_x a &\approx a^2\partial_x a\\
(a_d+b-1)^2\partial_x a &\approx b^2\partial_x a\\
(a+b_b)(a_d+b-1)\partial_x b &\approx ab\partial_x b
\end{aligned} \tag{A.7}$$

we find:

$$(\mathcal{L}\mathbf{\Psi}^\dagger)_1 = \partial_x\left[\partial_x^2 a + a - a^3 - \eta\, b^2 a\right] \tag{A.8}$$

Taking the derivative of (2.2) with respect to x we find that the right hand side of (A.8) is equal to zero when the amplitude solutions $a = a(x-r(t))$ and $b = b(x-r(t))$ are replaced by its form for $\delta = 0$. Hence, we conclude that $(\mathcal{L}\mathbf{\Psi}^\dagger)_1 = O(\delta)$. Likewise, we can prove that $(\mathcal{L}\mathbf{\Psi}^\dagger)_2 = O(\delta)$. Therefore, at lowest order in δ, $(\partial_x a,\ \partial_x b)^T$ belongs to the kernel of the operator $\mathcal{L}$.

Now we can calculate the evolution of the domain size $s(t) = d - 2r(t)$ through the solvability condition (A.5). We obtain:

$$\partial_t s \cong \pm 2v(\delta) + \frac{\int_{-\infty}^{\infty} dx(h_a\,\partial_x a + h_b\,\partial_x b)}{\int_{-\infty}^{\infty} dx[(\partial_x a)^2 + (\partial_x b)^2]} \tag{A.9}$$

where the coefficients h_a and h_b depend upon the amplitude solutions a and b and the non-potential parameter δ. The first term of the right hand side of (A.9) represents the rate of change of the domain size due to non-potential effects which cause the kinks to move at a constant velocity $v(\delta)$. The second term is related to kink interaction. In the case $\eta = 3$ we can compute explicitly all the coefficients involved in (A.9) taking advantage of the analytical kink profiles at lowest order in δ (equation (3.3)). Making an expansion in powers of $e^{-\sqrt{2}s(t)}$, retaining only the leading terms, and provided that δ is a small parameter, we obtain:

$$\partial_t s = \pm\frac{\delta}{\sqrt{2}} - 24\sqrt{2}e^{-\sqrt{2}s(t)} \tag{A.10}$$

which is eq. (3.10).

ACKNOWLEDGMENTS: Financial support from DGYCIT (Spain) Projects PB94-1167 and PB94-1172 is acknowledged.

[1] J. D. Gunton, M. San Miguel, and P. S. Sahni, in *Phase Transitions and Critical Phenomena*, edited by C. Domb and J. L. Lebowitz (Academic, London, 1983), Vol. 8.
[2] A. Bray, Adv. Phys. **43**, 357 (1994).
[3] P. C. Hohenberg and B. I. Halperin, Rev. Mod. Phys. **49**, 435 (1977).
[4] R. Montagne, E. Hernández-García, and M. San Miguel, Physica D **96**, 47 (1996).
[5] M. San Miguel and R. Toral in *Instabilities and Nonequilibrium Structures VI*, edited by E. Tirapegui and W. Zeller (Kluwer Academic Pub. 1997) and references therein.
[6] C. Josserand and S. Rica, Phys. Rev. Lett. **78**, 1215 (1997).
[7] L. Kramer, Z. Phys. B **41**, 357 (1981); L. Kramer, Z. Phys. B **45**, 167 (1981).
[8] P. Coullet and J. Lega, Phys. Rev. Lett. **65**, 1352 (1990).
[9] P. Coullet, C. Elphick, and D. Repaux, Phys. Rev. Lett. **58**, 431 (1987).
[10] S. Fauve and O. Thual, Phys. Rev. Lett. **64**, 282 (1990).
[11] E. Meron, Phys. Rep. **218**, 1 (1992).
[12] Y. Hu, R. E. Ecke, and G. Ahlers, Phys. Rev. Lett. **74**, 5040 (1995); Phys. Rev. E **55**, 6928 (1997).
[13] R. M. May and W. J. Leonard, SIAM J. Apl. Math **29**, 243 (1975).
[14] L. Frachebourg, P. L. Krapivsky, and E. Ben-Naim, Phys. Rev. E **54**, 6186 (1996).
[15] G. Küppers and D. Lortz, J. Fluid. Mech. **35**, 609 (1969).
[16] F. H. Busse and K. E. Heikes, Science **208**, 173 (1980).
[17] Y. Tu and M. C. Cross, Phys. Rev. Lett. **69**, 2515 (1992).
[18] M. C. Cross, D. Meiron, and Y. Tu, Chaos **4**, 607 (1994).
[19] A. D. Rutenberg and A. D. Bray, Phys. Rev. E **50**, 1900 (1994).
[20] T. Nagai and K. Kawasaki, Physica A **134**, 483 (1986).
[21] F. de Pasquale, P. Tartaglia, and P. Tombesi, Phys. Rev. A **31**, 2447 (1985).
[22] K. Kawasaki and T. Ohta, Physica A **116**, 573 (1982).
[23] P. Coullet, C. Elphick, and D. Repaux, Phys. Rev. Lett. **58**, 431 (1987).
[24] R. Toral and M. San Miguel (unpublished).
[25] A. C. Newell and J. A. Whitehead, J. Fluid Mech. **38**, 279 (1969).
[26] L. A. Segel, J. Fluid Mech. **38**, 279 (1969).
[27] G. H. Gunaratne, Q. Ouyang, and H. L. Swinney, Phys. Rev. E **50**, 2802 (1994).
[28] S.-K. Chan, J. Chem. Phys. **67**, 5755 (1977).
[29] B. A. Malomed, A. A. Nepomnyashchy, and M. I. Tribelsky, Phys. Rev A **42**, 7244 (1990).
[30] R. Montagne, A. Amengual, E. Hernández-García and M. San Miguel, Phys. Rev. E **50**, 377 (1994).
[31] We have checked on our numerical simulations, that on average, half the runs lead to a final state corresponding to a group of kinks moving to the right and half of them to kinks moving to the left.
[32] R. Gallego, M. San Miguel, and R. Toral (unpublished).

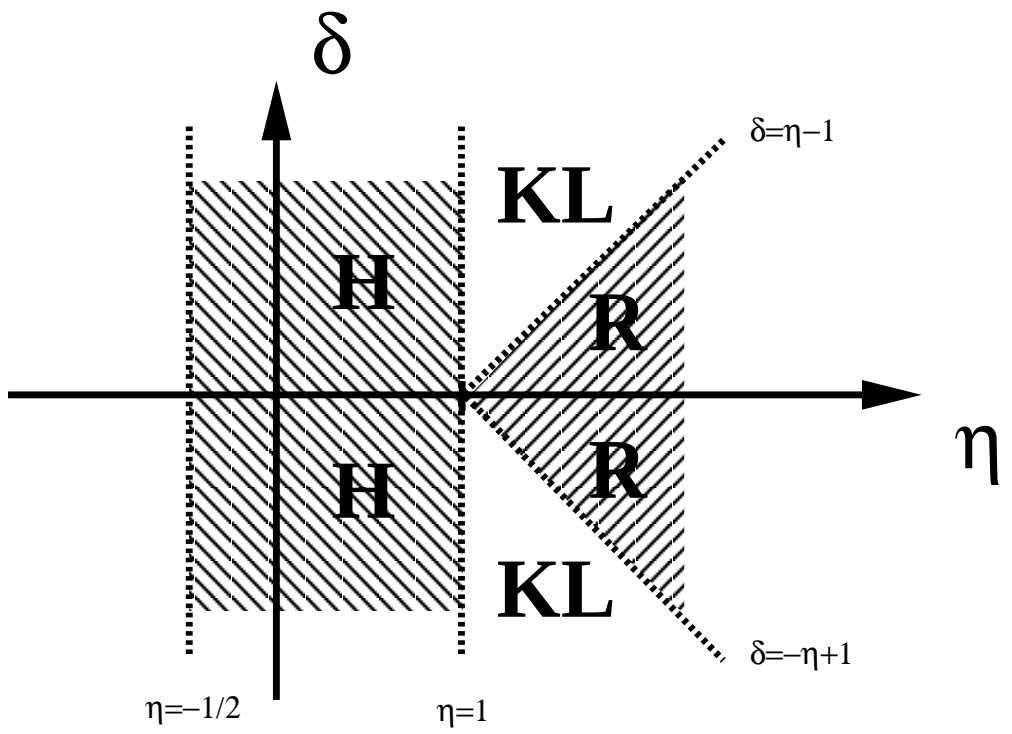


FIG. 1. Linear stability diagram of the homogeneous solutions of (2.2). Inside the region labeled with R, rolls are stable whereas in the H region, the stable solution is the hexagon. The KL region corresponds to the Küppers–Lortz instability.

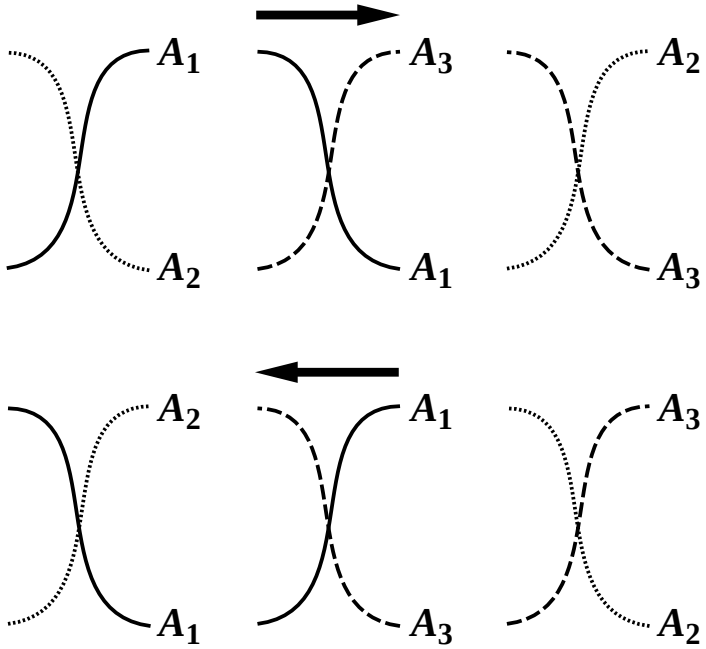


FIG. 2. Kinds of fronts and their direction of motion for $\delta > 0$. The remaining amplitude for each kink is understood to be zero across the interface. For $\delta < 0$ the picture is the same but with the arrows interchanged.

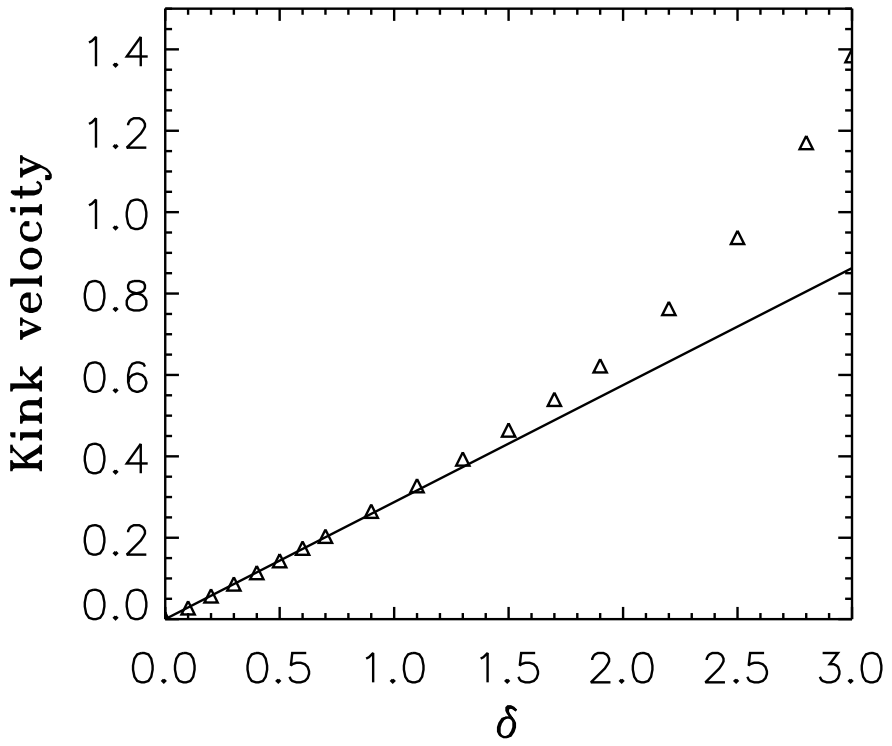


FIG. 3. Solitary kink velocity as a function of the non-potential parameter δ for $\eta = 3.5$. The straight line corresponds to the theoretical perturbative approach (3.9) whereas the points coming from numerical simulation.

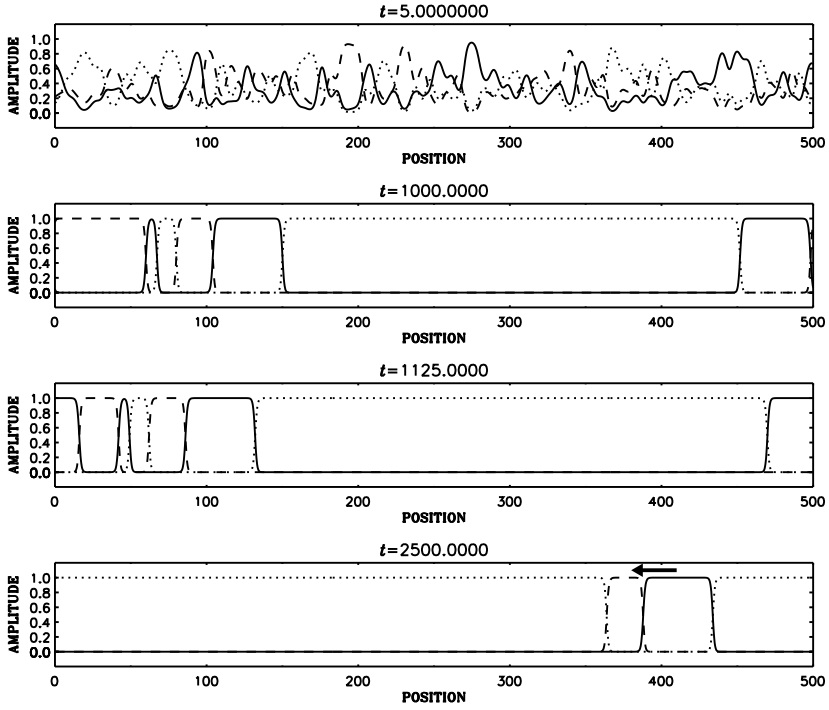


FIG. 4. Snapshots of the temporal evolution of the system. Parameter values: $\eta = 3.5$, $\delta = 0.5$, $L = 500$.

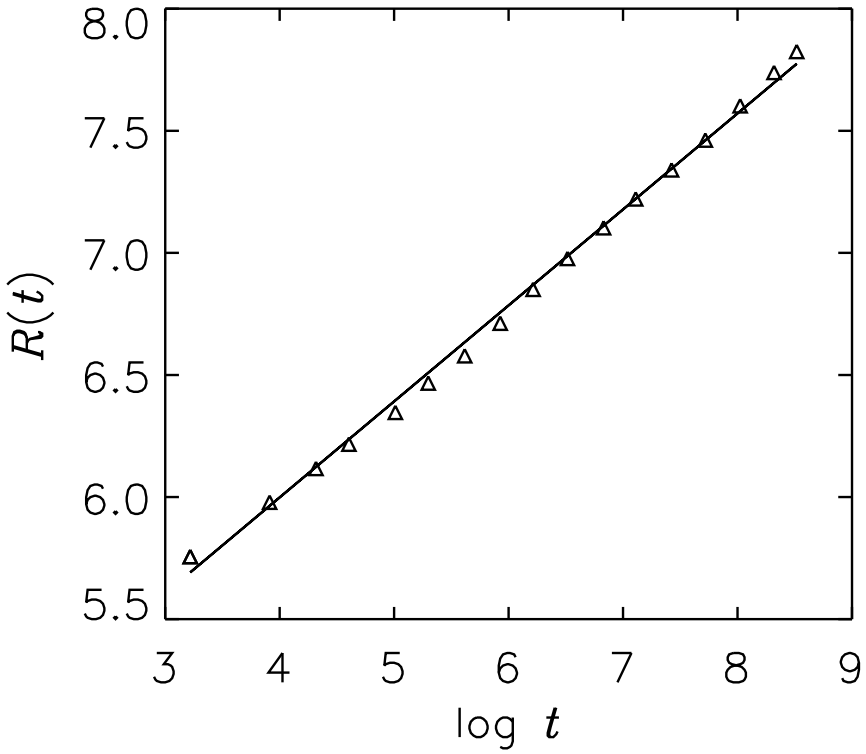


FIG. 5. Time evolution of the characteristic domain size for the potential case $\delta = 0$ and $L = 1000$. The straight line is a linear regression fit of points obtained numerically.

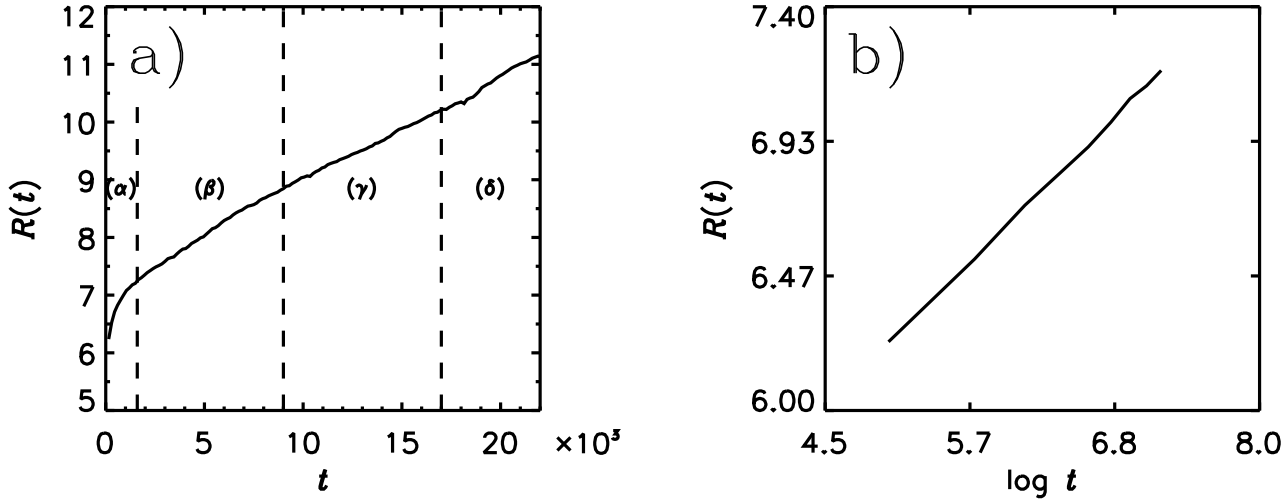


FIG. 6. (a) Time evolution of the characteristic domain size for $\delta = 0.001$ and $L = 1000$. The initial logarithmic growth law (region (α)) becomes linear (region (γ)) after a crossover (region (β)). Region (δ) is related to finite size effects. (b) Zoom of region (α) in the left plot with logarithmic time scale.

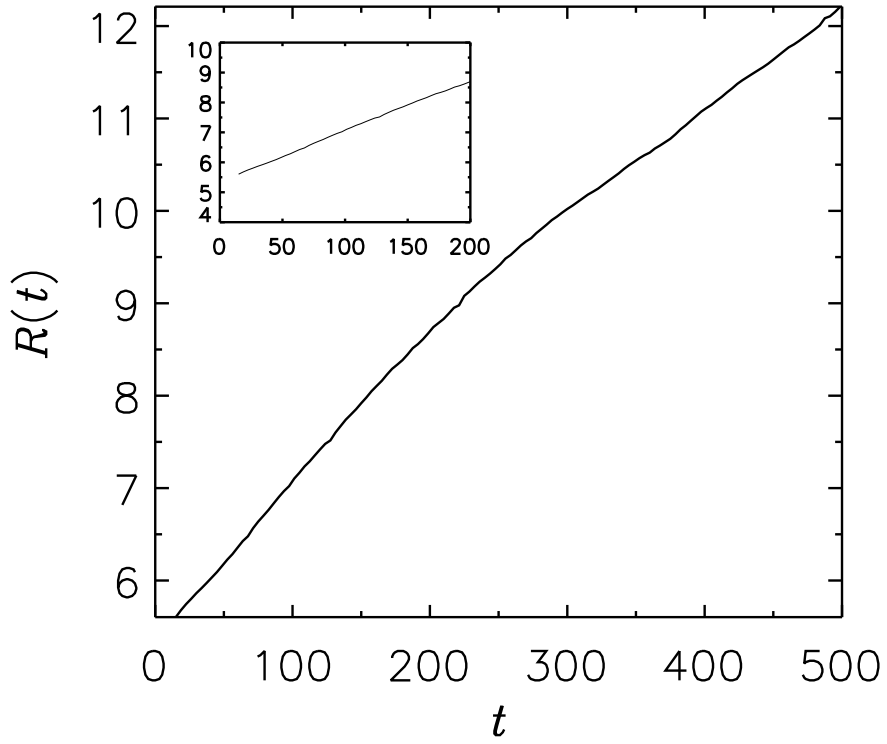


FIG. 7. Time evolution of the characteristic domain size for $\delta = 0.1$ and $L = 1000$.

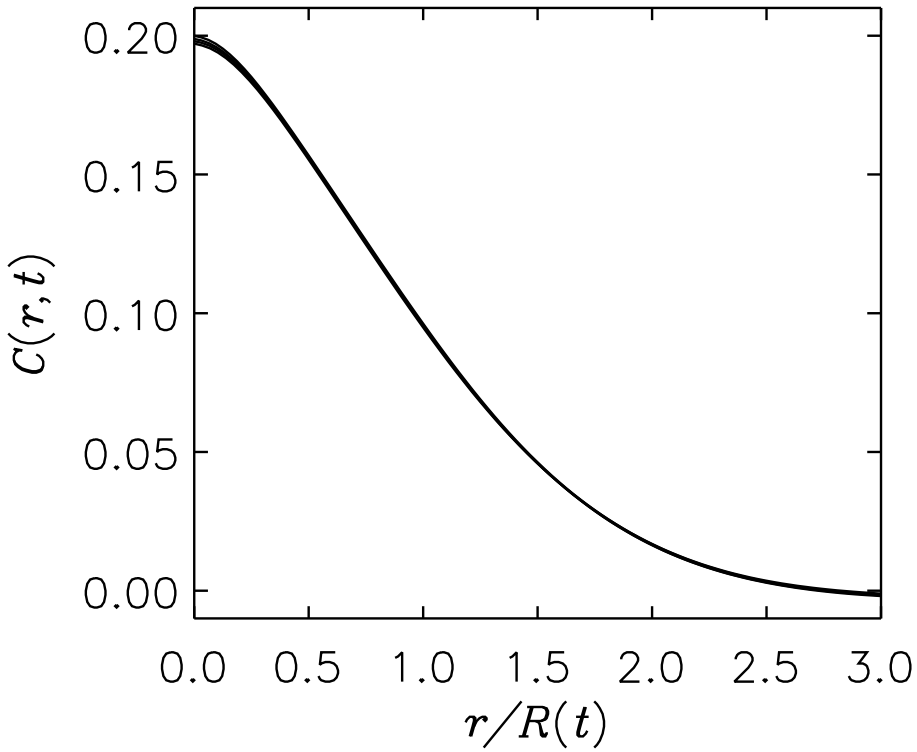


FIG. 8. Scaling function for the potential case $\delta = 0$. The plot has been made by over plotting $C(r, t_i)$ vs. $r/R(t_i)$ for several times from $t = 200$ up to $t = 5000$.

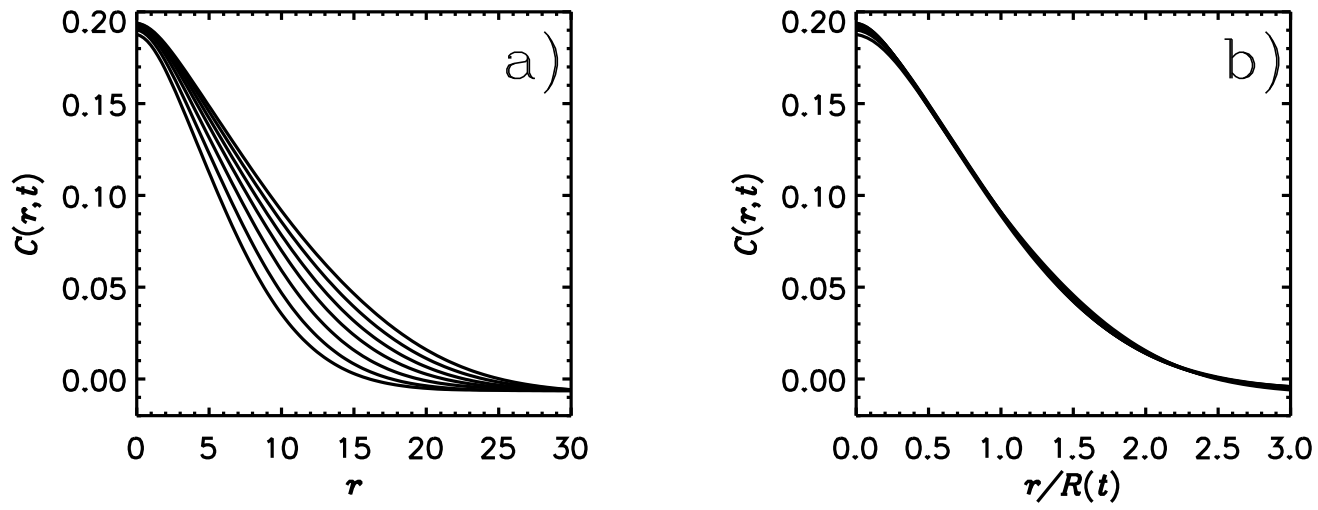


FIG. 9. (a) Equal time correlation function versus the non-scaled length for $\delta = 0.001$, $L = 1000$ and several different times from t=150 to t=15000. (b) Equal time correlation function versus the scaled length. The system parameters and the times for each curve are the same as in figure (a).

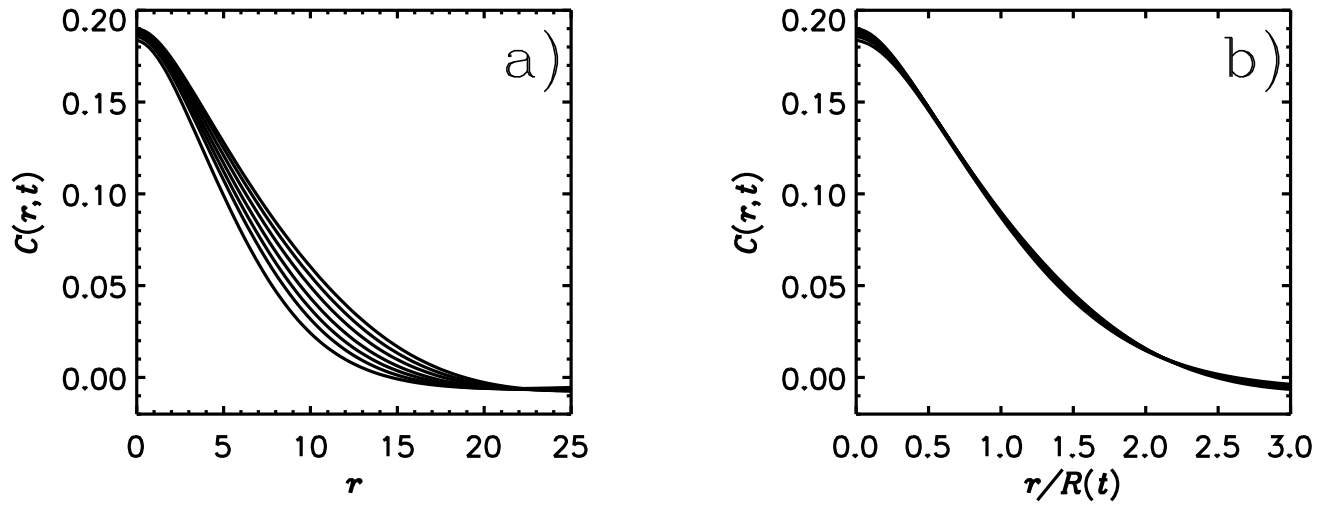


FIG. 10. (a) Equal time correlation function versus the non-scaled length for $\delta = 0.1$, $L = 1000$ and several different times from t=15 to t=150. (b) Equal time correlation function versus the scaled length. The system parameters and the times for each curve are the same as in figure (a).